University of Thi -Qar Journal for Engineering Sciences
http://www.doi.org/10.31663/tqujes.12.1.426(2022)
Vol 12.1 (April2022)

ISSN :2664- 5572 (online)
ISSN:2664-5564 (print)
Available at http://jeng.utq.edu.iq
utjeng@ utq.edu.iq

ANSYS method to the analysis of flow characteristics for the elbow of an oil pipeline

Enas Ramadhan Khalaf[a], Hussam Ali Khalaf[b] .
[a,b]. Mechanical Engineering Department, Collage of Engineering, University of Thi-Qar , Iraq.

Abstract

The flow of oil-water mixture in a pipeline can take place in a variety of patterns. It's appear during the transportation of oil and in wellbore. The fraction of water in the output stream will increase as the producing life of a well increases. Being able to estimate the pressure loss in such systems is critical for properly designing the conveying system. In this study the ANSYS fluent 2021 R2, the VOF method the RNG, k- model were used to simulate three dimensional turbulent flow of the oil-water flow in elbow pipe of 55.57mm diameter and straight pipes at its two side of 800mm length with three water volume fractions 25%, 50%, 75%. The flow pattern and the distribution of the velocity and the influence of the elbow angle on them were studied. Also prediction of the pressure drop and the effect of water volume fraction and the influence of elbow angles on it. The result show that the pressure drop increase by increasing the water volume fraction, and the largest pressure drop happened at 90° elbow angle while the lowest at 45°.

Keywords: VOF, oil-water, two phase flow, pressure drop, elbow

1. Introduction

An oil-water system presents complex and unique problem in pipeline transportation of the crude oils in the industry of petroleum due to its unusual rheological behavior. Type of flow pattern is a common observation in this field of studies because even slight differences in flow conditions will exhibit different flow configurations. In multiphase flow system even more important thing to discuss is about pressure. Both flow pattern and pressure were actually directly related since both are dependent under the same factors such as density ratio, mixture flow rate, wetting properties, surface tension, viscosity ratio and etc.**[1]**. The immiscible liquid-liquid flow common in the chemical industries, petroleum engineering and ocean engineering, as well as the process of transportation**[2].**

[3] investigated the oil–water flow in stainless steel straight pipe in cross section with 50 m and 25.4 mm length and ID, respectively. For low water percentages and mixing velocities, this took up the whole cross section of the pipe. When the volume fraction or velocity of water rose, it seemed to separate. The water-in-oil mixture produced an annular flow in large water percentages and mixing velocities, in the center and encompassed by water. The finding obtained were compared to a similar viscosity model oil. The patterns obtained oil systems defined by water separation dispersed with increased mixture velocity or water fraction were comparable at low water percentages. However, at significant water fractions, the model oil produced diffusion that the crude oil did not. The pressure decrease in the crude oil system was typically larger than in the model system, although it fell in both situations When water began to separate and create layers at the pipe's contact. **[4]** has investigated by (CFD) for single and two phase flow in a 90 °elbow horizontal - vertical with a 12.7 mm inner diameter, behavior of the elbow was studied at six distinct upstream and downstream sites. During this investigation, three distinct velocities for air and three different velocities for water were employed to examine the impacts of different phases. The pressure drop behavior of single-phase and multiphase flows was observed to be similar. A comparison of CFD findings with available empirical models revealed that they were pretty good**. [5]** have investigated what is the significance of the influence of a little reduction in diameter of the pipe on pressure gradient and flow patterns in 19 mm ID pipe. The results show a notable influence of diameter of the pipe on the gradient of pressure and flow patterns. The region for both continuous and scattered oil in water flows grows as the diameter of the pipe grows from 19mm to 25.4 mm, whereas the amount of stratified, annular flow and bubble zones decreases. At identical surface oil and water velocities, the values of pressure gradient recorded in the pipe of 19 mm are larger than those found in the pipe of 25.4mm. With increasing the velocities of oil & water, the disparities in pressure gradient become more pronounced**. [6]** have investigated the fluid flow in a 90 ° angle curved pipe with a large curvature ratio as a preliminary research and simulation. A turbulence model, DES was utilized to examine fluid flows with Reynolds numbers ranging (5000 - 20000). The result indicate that fluid flow in a curved pipe with a high curvature ratio differs from fluid flow in a curved pipe with a small curvature ratio. Separation region, The flow patterns and oscillating flow are all varied because a large curvature ratio complicates internal flow. **[7]** have simulated two-phase flow in a 0.0254m horizontal pipe. Used volume of Fluid (VOF) with turbulence model RNG k- to simulate the stratified flow regime. The velocity effect on the gradient of pressure was also studied. 0.2 m/s, 0.5 m/s, 0.8 m/s and 1.1 m/s . Presented Using the

proper multiphase model and turbulence model, flow velocity with the same volume fraction for each phase.

[8] determined the characteristics of flow separation in high Reynolds number pipe bends to investigate one phase turbulent flow across pipe bends. The numerical results show that flow separation is easily visible for bends with a small curvature ratio. The velocity patterns obviously demonstrate the secondary motion induced by fluid transfer from the inner wall to the outer of the bend, resulting in flow separation. **[9]** have established a physical model of a 90º bend pipe with diameters of 27.3cm, 37.7cm, and 42.6cm, and analyzed numerically the error of flow measurement in various measuring location after elbow by using finite volume method. The results indicate that the upstream in elbow produces local fluid disruption, resulting in a quasi-distribution of fluid velocity in the downstream pipeline, which has a considerable impact on the flow measurement variance an the accuracy of supersonic measurement of flow at different points. When pipe radius increases, the degree of fluid flow velocity variation decreases, but the accuracy of flow measurement diminishes. The wider the pipe diameter in the whole range of flow measurement, the narrower the fluctuation period of a relative error. Specifically, improved the precision of flow measurement

[10] have studied numerically the factors influencing and encouraging displacement of water at the elbow of a horizontal-upwardly inclined pipeline with diesel oil and a 27 mm inner pipe diameter 3D. As the restricted volume rises, the minimum oil speed required to initiate water displacement lowers. With increasing superficial velocity, velocity of water increases in a straight line. **[2**] evaluated the oil–water flow in three distinct elbow configurations to explore the corrosion-prone properties of elbow designs and used the (VOF) approach and the (RNG), k- model. For all configurations of flow, the highest mass transfer coefficient and shear stress of the wall are found at the intrados of the elbow. Nonetheless, water does not directly interact with the elbow's intrados in horizontal-upward and horizontal-horizontal, making it far less corrosive. When all this was complemented with a water wetting process study, it was determined that the horizontal-downward elbow flow had the highest corrosion danger The horizontal-upward elbow flow was the lowest of the three tested designs, while the horizontal-horizontal elbow flow was in the center.

2. Mathematical modeling

The VOF is simple, effective approach was used to model the oil–water elbow flow because it solves the equations of momentum and records the volume percentage of fluid in a control body.

Fig.1 Oil pipeline

2.1. Assumptions of flow:

The assumptions were made through the building of the mathematical model as follow:

1. Two phase flow
2. Unsteady state (transient) and turbulent flow.
3. Non slip flow.
4. The two fluids is incompressible with constant properties.
5. Newtonian flow.

2.2. Governing equations:

2.2.1 The model equations:

The following are the continuity, momentum, and volume fraction equations used in the calculations [11],

$$\frac{\partial \rho}{\partial t}+\nabla.(\rho u)=0, \quad (1)$$

$$\frac{\partial \rho u}{\partial t}+\nabla(\rho u \times u) = -\nabla p + \rho g + [\mu(\nabla u+\nabla u^{T})] + F, \quad (2)$$

$$\frac{\partial \rho_o \alpha_o}{\partial t}+\nabla.(\rho_o \alpha_o u)=0, \quad (3)$$

The volume of the mixture is equal to the total of the volumes of the components, as follow:

$$\alpha_w+\alpha_o=1, \quad (4)$$

and the density of the mixture may be stated as follow:

$$\rho_m=\alpha_o\rho_o+\alpha_w\rho_w , \quad (5)$$

where:

Linear combination equation was adopted to calculation the viscosity of the mixture:

$$\mu_m=\alpha_o\mu_o+(1-\alpha_o)\mu_w , \quad (6)$$

The surface tension equation between the two phase considered as:

$$F= \sigma_k \frac{\rho \nabla \alpha_o}{\frac{1}{2}(\rho_o+\rho_w)}, \quad (7)$$

$$\kappa=\nabla \bullet \hat{n}, \quad (8)$$

n : the surface normal vector.

$$\hat{n} =\frac{n}{|n|}, \quad (9)$$

which defined as the gradient of the oil volume fraction

$$n=\nabla\alpha_o, \quad (10)$$

where;

κ : the curvature.

n^: the unit vector.

The following equation may be used to substitute the normal vector of the unit surface of the unit body adjacent to the wall :

$$\hat{n}=\hat{n}w\cos\theta_w+\hat{t}w\sin\theta_w, \quad (11)$$

2.2.2. Turbulence model

To predict whether a flow condition is laminar or turbulent, the Reynolds number (Re) is used, which indicates the ratio of inertial forces to viscous forces,

$$Re=\frac{\rho u D_h}{\mu}, \quad (12)$$

Where: Dh is the hydraulic diameter.

The RNG k-ε model was adopted, because of its accuracy, and economy across a wide range of topics of turbulent flows, standard k-ε is widely used in industrial flows, which explains its popularity and its equation is as follows:

The turbulent kinetic energy:

$$\frac{\partial}{\partial t}(\rho k)+\nabla\bullet(\rho k u) = \nabla \bullet [(\alpha k \mu_{eff})\nabla \bullet k] + G_k + G_b - \rho\varepsilon - Y_M + S_k , \quad (13)$$

The specific dissipation rate:

$$\frac{\partial}{\partial t}(\rho\varepsilon)+\nabla.(\rho\varepsilon u) = \nabla.[(\alpha\varepsilon\mu_{eff})\nabla.\varepsilon] + C_{1\varepsilon}\,\varepsilon\frac{\varepsilon}{k}(G_k + C_{3\varepsilon}\ C_b) - C_{2\varepsilon}\varepsilon\frac{\varepsilon^2}{k} - R\varepsilon + S\varepsilon, \quad (14)$$

$$\mu_{eff}=\mu+\mu_t, \quad (15)$$

$$\mu_t=\rho\, C_\mu \frac{K^2}{\varepsilon} \quad (16)$$

where μ_{eff} is the effective viscosity, μ_t is the turbulence viscosity, and the value of $C_{1\varepsilon}$and $C_{2\varepsilon}$ are 1.42 and 1.68, respectively. C_μ is 0.0845, [12].

To calculate the total pressure drop, the following equation is used:

$$\Delta P=P_2-P_1 \quad (17)$$

The volume fraction was determined using the geometric restructuring technique, and the momentum, turbulent kinetic energy, and turbulent dissipation rate were all computed using a second-order discretization methodology in FLUENT, transient, explicit calculation and the time step was adjusted to 0.01 s.

3. Numerical method

3.1 Boundary condition:

- The inlet boundary conditions are as follows: The mixture velocity is 1 m/s and the αw is 25%, the two fluids enter separately to the pipe
- The wall boundary conditions are as follows: The wall is no-slip boundary condition.
- The outlet boundary conditions are as follows: The outlet pressure is 0 MPa.

3.2 The properties of fluids:

Table (1) shows the physical properties of the fluids utilized in this work[12]

Table 1.The oil and water properties

Parameter	Value
ρ_o	790 kg/m3
ρ_w	1000 kg/m3
μ_o	0.0016 Pa.s
μ_w	0.00103 Pa.s
σ	0.043 N/m

3.3.Geometry creation:

The Fluent's initial step in simulation is to create or draw the geometry of the investigated model or problem. This process is carried out with the help of ANSYS Workbench, which is a software environment for creating geometry and generating the needed mesh, as well as performing thermal, structural, and electromagnetic studies. In this thesis, the ANSYS Workbench 2021,R2 software was used to draw and generate the appropriate mesh for the elbow pipe model. The ANSYS Workbench of program includes a wide range of capabilities for drawing simple and complicated geometries.

3.4. Creating meshes:

After designing the analyzed model, the second needed step for completing the CFD simulation is to generate the appropriate mesh. Creating a polyhedral or polygonal mesh that approximates the geometric domain is known as mesh generation. Because of the many usage of computational mesh in physical simulations such as finite element or computational fluid dynamics to solve three-dimensional continuity, momentum, and energy equations, it has always been the topic of intense researches. For this study, ANSYS Workbench 2021,R2 was used, which includes a variety of meshes such as hexahedral and tetrahedral, as well as structured and non-structured meshes. as seen in the **fig. (2).**

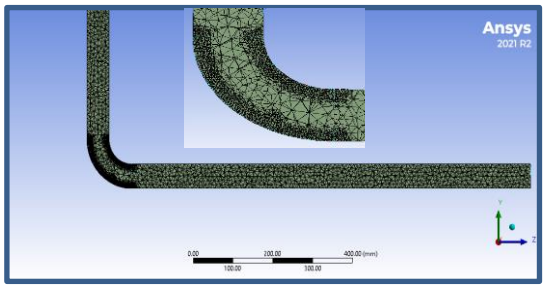

Fig.2 Mesh generation.

3.5. Mesh convergence test

In order to get a reliable results and do not depend on the mesh size of the model a number of mesh size has been taken until a convergence has been obtained. Figure below shows the convergence of the maximum pressure in the pipe with mesh number. As shown the curve after 82904 mesh elements the curve became nearly horizontal. Which mean that the maximum pressure or the solution results no more dependent on the mesh size. Also the percentage change in the results between two results obtain in to different mesh size. It is value was 18% between mesh1 and mesh2, 23% between mesh2 and mesh3, 4.9% between mesh3 and mesh4 and 2.5% between mesh4 and mesh5 which is an acceptable value and fall in the range of the acceptable tolerance for the mesh which is (1-5)%.

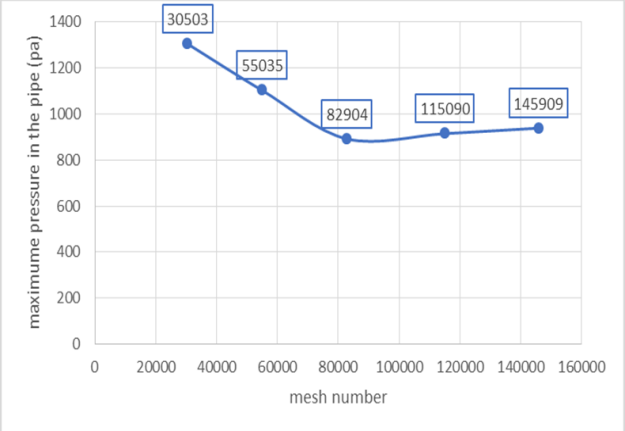

Fig.3 Comparison of the different numbers of grid used to the model.

The percentage change was calculated according to the equation

$$\text{percentage change} = \frac{(\phi\_(at\ first\ mesh\ - \phi\_(at\ second\ mesh)}{\phi\_(at\ first\ mesh)} \times 100\%$$

Where: ϕ is a result variable, which is the pressure in this case.

Table 2 List the value of the maximum pressure, mesh number and the percentage change.

Mesh	Number of elements	Maximum pressure (pa)	Percentage change %
Mesh1	30503	1305	
Mesh2	55035	1103	18%
Mesh3	82904	892.2	23%
Mesh4	115090	915.2	4.9%
Mesh5	145909	939.1	2.5%

4. Results and Discussion

4.1.The verification:

The current simulation process was validated with [2]. Where the same model dimensions and fluids properties are repeated for the same process. The reference paper used oil and water flow in 90 degree elbow with mixture velocity of 1.05 m/s and the entrance split to two regions. The water volume fraction was 0.25 in inlet2. Also the plane where the results was taken is at the start of the elbow. The comparison of the results shows 4% difference between the current results and the reference paper. this difference comes because the difference between the time step size where in the current simulation the time step size was 0.001 where it was 0.0001 in the paper and also because of the difference in the grid distribution, where in the paper used inflation layer has 0.1 mm thick near the wall , in the current simulation these was not used because it is time-consuming and require a higher computational time so it was ignored.

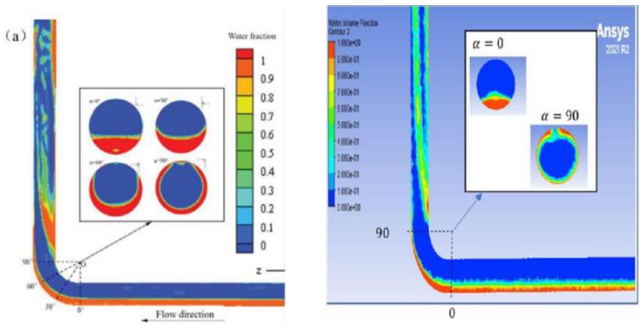

Fig.3 Distribution of :(a) Water volume fraction in the paper [2] (b) Water volume fraction in this thesis

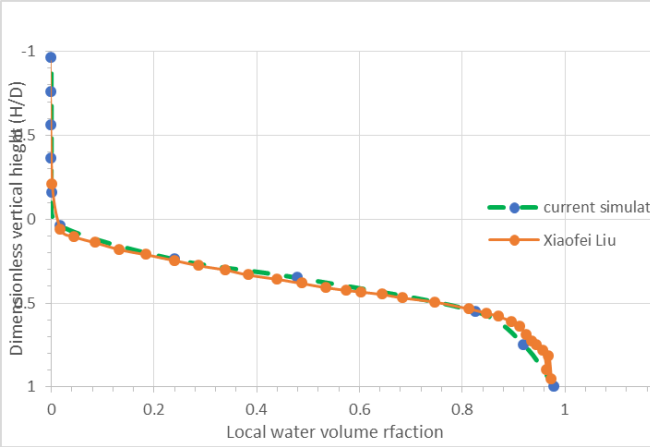

Fig.4 Comparison of the current study results and that of [2] for the water volume fraction with the dimensionless number high.

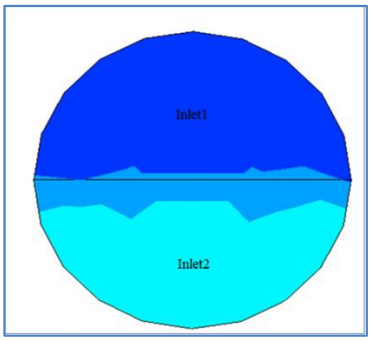

Fig.5 The configuration the inlet of the pipe in current study and [2]

4.2. Distribution of water volume fraction.

At inlet velocity of mixture 1m/s, and 25% water volume fraction, figs.(6) the flow in the horizontal pipe is stratified where the oil is flow over the water due to its low density and there is slight water dispersing into the oil. The flow pattern in the elbow was annular where the water formulas a layer around the walls of pipes and the oil in the center. In the vertical pipe the flow start to be rotational due to the change of momentum when the velocity change its direction, where the elbow work as a deflector to the velocity.

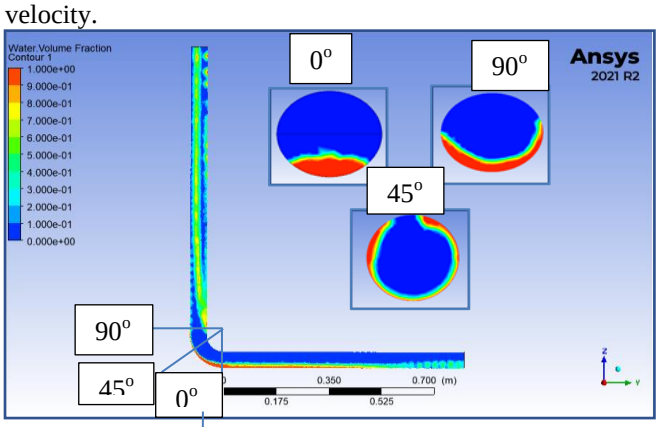

Fig.6 The contour of distribution of water fraction α_W =25%.

At the same inlet velocity of mixture 1m/s, and 50% water volume fraction, there was no big different in the result of previous case in horizontal pipe which is stratified and the elbow where the flow was semi-annular. In the vertical pipe, when the water is squeezed out of the tube's center, it forms a thin film on the wall (form in a ring of water). As shown in fig.(7).

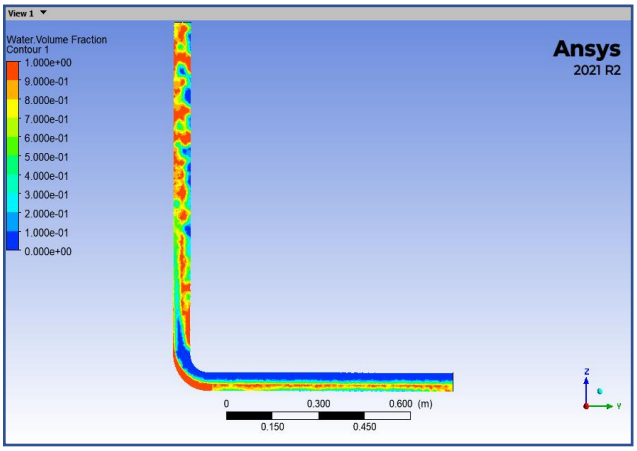

Fig.7 The contour of distribution water fraction α_W=50%.

When the water volume fraction is 75%, at the same inlet velocity of mixture 1 m/s, the flow in the horizontal was stratified with water droplet, the flow pattern in the elbow also annular shape but the water layer is thicker than this in the previous cases and the intrados are not wet with water, under the influence of gravity, water would fall back into elbows, forming a stagnant water region. In the vertical pipe the centrifugal force spilled the water to the wall but also due to the gravity which its direction is opposite to the gravity centrifugal force the oil dispersed in the water.

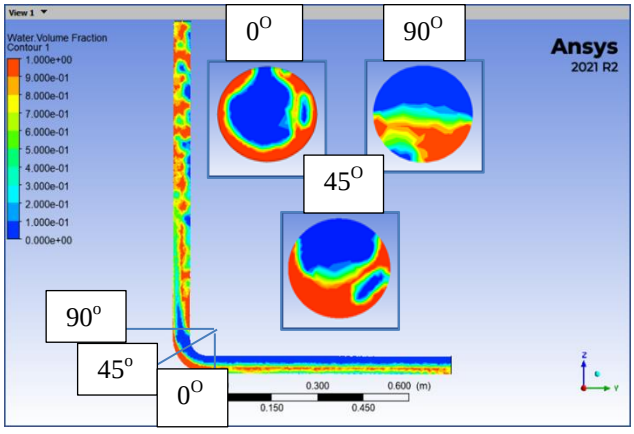

Fig.8 The contour of distribution of water fraction α_w=75% .

At the inlet mixture velocity 2m/s, and elbow angle 67° and 25% water volume fraction, the flow in the horizontal pipe is wavy stratified with mixing layer of oil and water at the interface, in the elbow the flow is semi-annular due to the centrifugal force, in the vertical pipe the flow is rotational flow and its pattern is wavy stratified. As shown in fig.9.

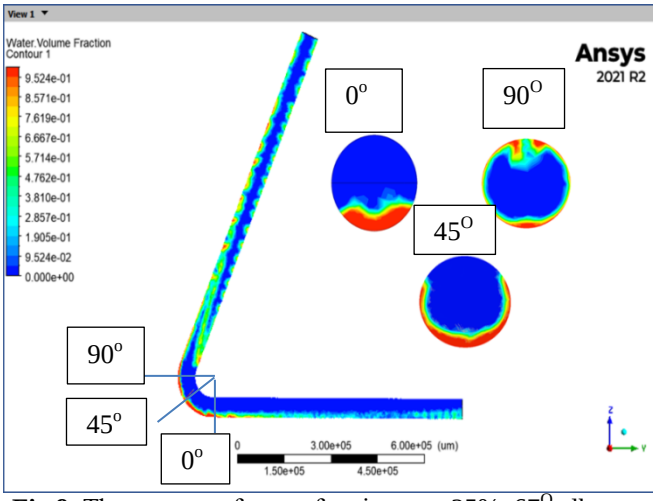

Fig.9 The contour of water fraction α_w =25% ,67^O elbow angle and inlet mixture velocity 2m/s.

At the inlet mixture velocity 2m/s, 90^o elbow angle 25% water volume fraction the flow in the horizontal pipe is wavy stratified with mixing layer of oil and water at the interface, in the elbow the flow is semi-annular due to the centrifugal force, in the vertical the water is very thin layer on the wall and then a layer of dispersed oil in water and the oil in the center. As shown in fig.(10). The buoyancy impact was still significant in comparison to the inertia effect, and a clear water layer flowed through the conduit's bottom part. With the rise in oil percentage, the thickness of this water layer reduced.

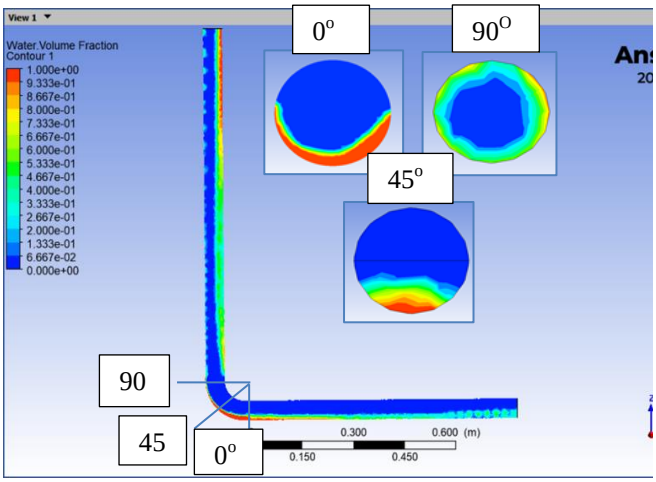

Fig.10 The contour of water fraction α_w =25%, 90^O elbow angle and 2m/s inlet mixture velocity.

4.3..Distribution of velocity

The distribution of the velocity for 1m/s inlet mixture velocity,25% water volume fraction at 90^o elbow angle presented in Fig.11, the mixture velocity at the walls is zero, in the horizontal pipe the velocity increase gradually toward the center of pipe. The maximum values occur at the intrados of the elbow and in the vertical pipe at the outer wall due to the washing of the oil phase.

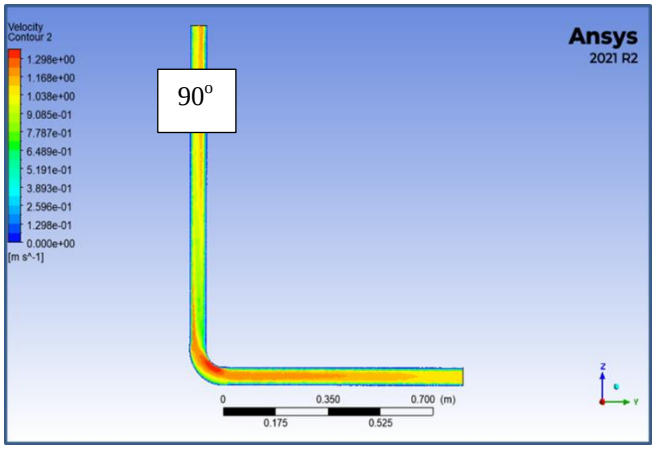

Fig. 11 Distribution of velocity at α_W =25%, inlet mixture velocity 1m/s.

When the water volume fraction is 50%, the distribution of the velocity for 1m/s inlet mixture at 90^o elbow angle presented in Fig.12, the mixture velocity at the walls is zero, in the horizontal pipe the velocity increase gradually toward the center of pipe. The greatest values are seen at the elbow's intrados. and in the vertical pipe at the outer wall due to the washing of the oil phase.

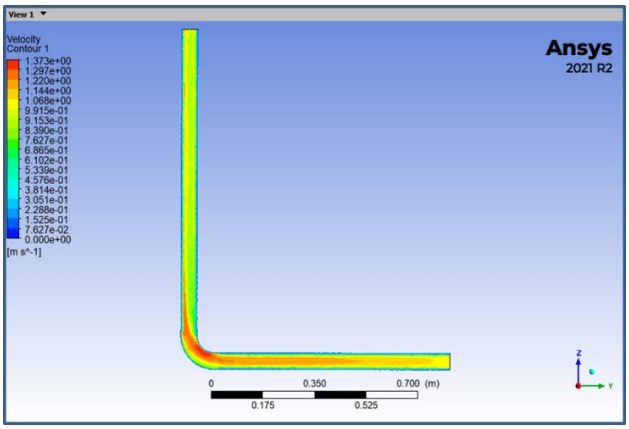

Fig. 12 Distribution of velocity at α_W =50%, inlet mixture velocity 1m/s.

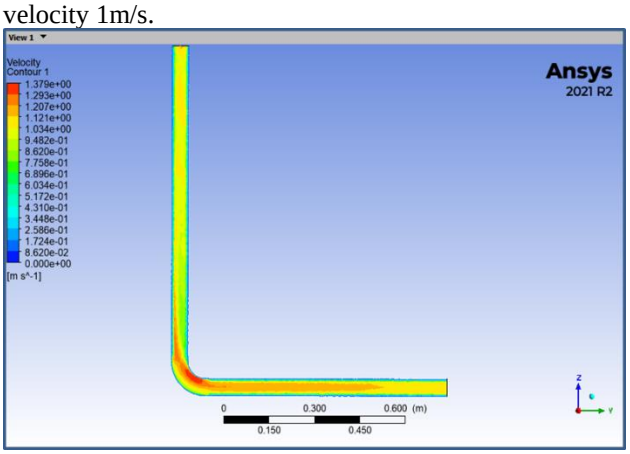

Fig.13 Distribution of velocity at α_W =75%, inlet mixture velocity 1m/s.

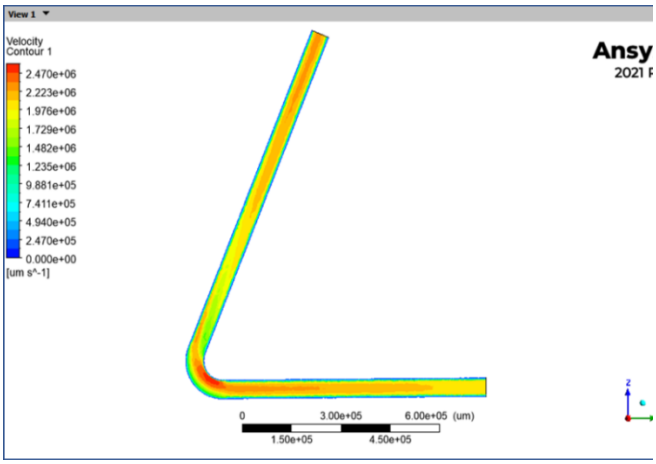

Fig.14 Distribution of velocity at α_w =25%, 67^O elbow angle, inlet mixture velocity 2m/s.

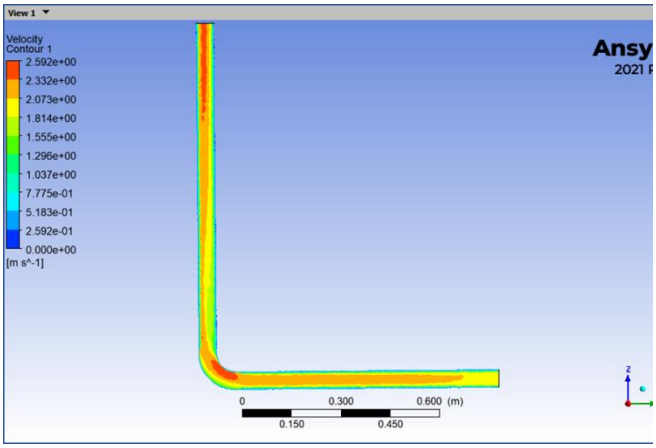

Fig.15 Distribution of velocity at α_w =25%, 90^o elbow angle, inlet mixture velocity 2m/s.

4.4. Distribution of pressure.

The distribution of pressure when the water volume fraction is 25% at three elbow angles (45^o, 67^o, 90^o) degree shown in figs,(16),(17),(18). The pressure in the horizontal pipe at its maximum value at the beginning of the pipe and it is gradually decrease due to frictional pressure drop in the pipe. And it's at its maximum value at the extrados of the elbow. In the pipe after elbow, the pressure start decrease due to the vortex flow and backflow and it's reach its minimum value at the end of the pipe.

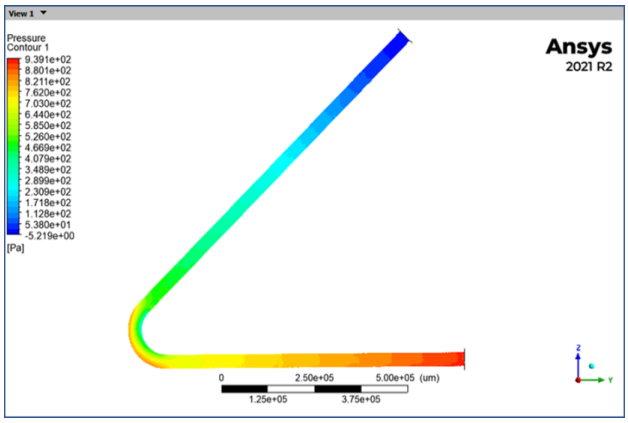

Fig.16 Distribution of pressure in 45^o degree elbow, α_w =25%.

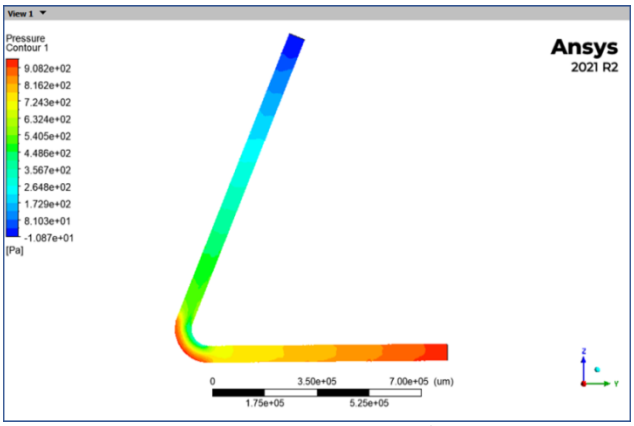

Fig.17 Distribution of pressure in 67^o elbow angle, α_w= 25%.

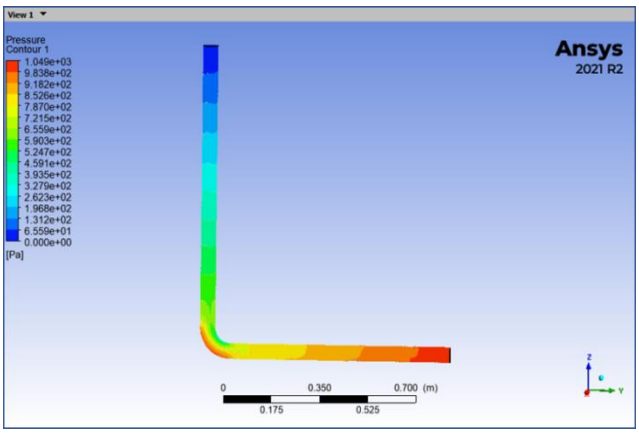

Fig.18 Distribution of pressure in 90^o elbow angle, α_w= 25%.

The relation between the pressure drop in the pipe and the elbow angle with constant water volume fraction α_w= 25%. shown in the fig.19. The lowest pressure drop happens at 67^o elbow angle, but the highest at 90^o .

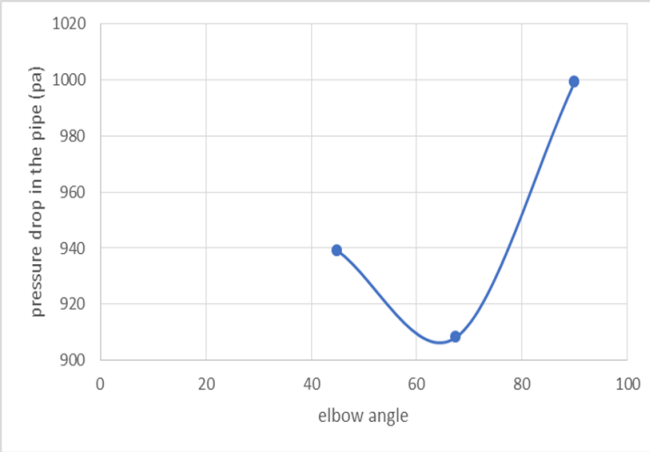

Fig.19 The relation between the pressure drop in the pipe and the elbow angle.

Then the effect of water volume fraction on pressure drop with one elbow angle (90^o) is studied . The water volume fraction (25%,50%, 75%) are studied and the result shown in the figs.(20),(21),(22). The pressure distribution in the fig.(4-19) show that the flow which inter the pipe is at its maximum value of pressure and then decrease in the straight pipe , when it enters the elbow there is two region of pressure, high pressure region at the extrados and low pressure at the intrados. Because the change of direction of flow due to the centrifugal force the pressure at the downstream decrease until reach to the outlet pressure (0 Mpa).

The fig.(20) shows the distribution of pressure in 90 degree elbow, α_w =25%, which it decrease along the pipe.

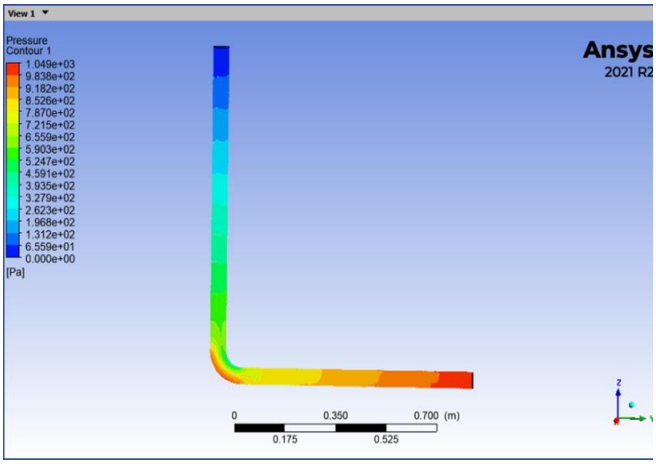

Fig.20 Distribution of pressure in 90^o degree elbow, α_w =25%.

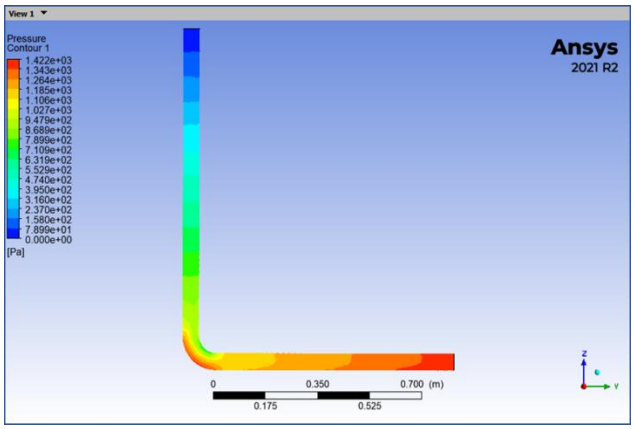

Fig.21 Distribution of pressure in 90^o degree elbow, α_w =50%.

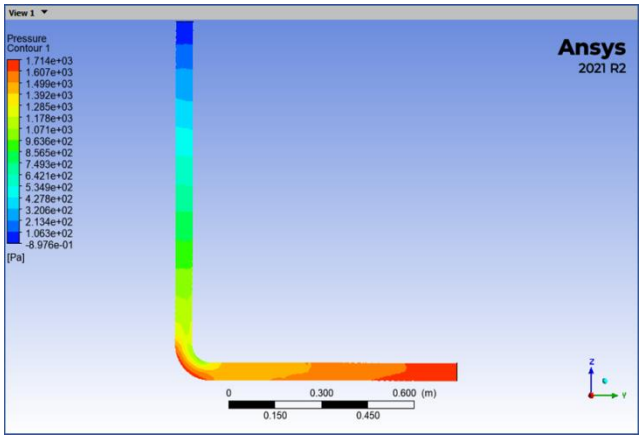

Fig.22 Distribution of pressure in 90^o degree elbow, αw =75%.

The fig.(23) shows the relation between the water volume fraction and the pressure drop which it's increase by increasing of water volume fraction.

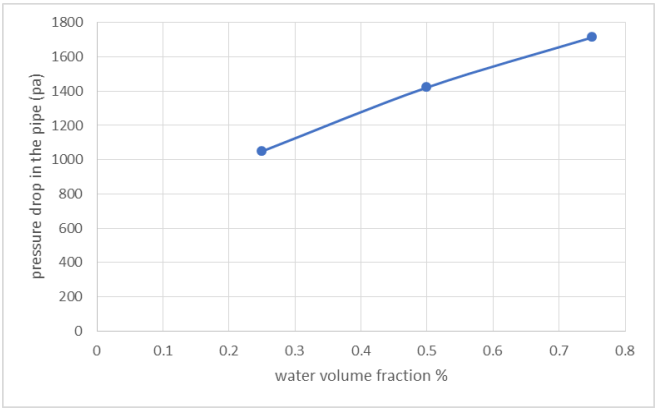

Fig.23 The relation between the water volume fraction and the pressure drop.

5. Conclusions

In this study, the ANSYS fluent 2021 R2, the VOF method the RNG k-ε model were used to simulate three

dimensional turbulent flow of the oil and water flow in elbow pipe.
The numerical method's accuracy was verified by comparing the findings to existing data. The results displayed reasonable agreement. after which they investigated the flow characteristics.

The following are the main conclusions:

1. In all three water volume fraction, The flow in the horizontal pipe is stratified where the oil flows over the water due to its low density, and there is slight water dispersed into the oil. At the elbow, the flow becomes annular gradually due to the influence of the centrifugal force. In the vertical pipe, the flow was rotational due to the change of momentum when the velocity changes its direction, where the elbow works as a deflector to the velocity.
2. The mixture velocity at the walls is zero. In the horizontal pipe, the velocity increases gradually toward the center of the pipe. Maximum values are found at the elbow's intrados and the vertical pipe's outer wall.
3. The pressure distribution at 45o, 67o, and 90o degree elbows when the αw is 25% is high at the entry and gradually decrease as it flows towards the pipe's exit. During the extrados, it was at its maximum value.
4. The pressure drop directly proportional to the water volume fraction

Abbreviations :

Symbol	Definition	Unit
C1	Coefficient in equation	
C2	Coefficient in ε equation	
C3	Coefficient in ε equation	
D	Diameter of pipe	m
G_k	Generation of turbulent kinetic energy due to mean Velocity gradient	$N.m^{-3}$
G_b	Generation of turbulent kinetic energy due to buoyancy	$m.\ s^{-2}$
F	Surface tension term	$m.\ s$
g	Acceleration of gravity	$m^2.s^{-2}$
G	Generation of turbulence kinetic energy,	m
K	turbulence kinetic energy	m^{-1}
L	Length	m^{-1}
n	Unit normal vector to a surface	m^{-1}
$\hat{n}$	Unit normal vector	pa
$\hat{t}$	Unit tangent vector	
P	Pressure	$m.s^{-1}$
Re	Reynolds number	$kg.m^{-2}.s^{-2}$
U	Velocity	$Kg.m^{-2}.s^{-2}$
S_k	User-defined source term	
S_ε	User-defined source term	
YM	Contribution of fluctuating dilatation in compressible turbulence to overall dissipation in Compressible turbulence affecting overall dissipation rate.	Kg.m-3
Greek Symbols		Pa
ρ	Density	
μ	Viscosity	
σ	The surface tension coefficient	
α	Phase volume fraction	
α_k	Inverse effective Prandtl number for k	
α_ε	Inverse effective Prandtl number for _ε	

References

[1] Beden S. M., "Reliability of the Installation and Operation of Pipeline Systems*",* Basrah Journal for Engineering Sciences, 2016, 2, 108.

[2] Xiaofei Liu, Chengcheng Gong, Lite Zhang, Haozhe Jin and Chao Wang, "Numerical study of the hydrodynamic parameters influencing internal corrosion in pipelines for different elbow flow configurations", 2020 ,14, 122.

[3] Wei Wang, Jing Gong and Panagiota Angelic, "Investigation on heavy crude-water two phase flow and related flow characteristics", 2011, 37, 1156.

[4] Quamrul H. Mazumder," CFD Analysis of Single and Multiphase Flow Characteristics in Elbow", University of Michigan-Flint, 2012, 4.

[5] T. Al-Wahaibi, Y. Al-Wahaibi, A. Al-Ajmia, R. Al-Hajri N. Yusuf, A.S. Olawale and I.A. Mohammed, "Experimental investigation on flow patterns and pressure gradient through two pipe diameters in horizontal oil–water flows", 2014, 122, 266.

[6] Yan Wang, Quanlin Dong, Pengfei Wang, "Numerical Investigation on Fluid Flow in a 90-Degree Curved Pipe with Large Curvature Ratio", 2015.

[7] Adib Zulhilmi Mohd Alias, J. Koto and Yasser Mohamed Ahmed, "CFD Simulation for Stratified Oil-Water Two-Phase Flow in a Horizontal Pipe",2015,2.

[8] Prasun Dutta, Sumit Kumar Saha, Nityananda Nandi and Nairit Pal, "Numerical study on flow separation in 90° pipe bend under high Reynolds number by k-ε modeling", Engineering Science and Technology an International Journal, 2015, 2, 20.

[9] Songsong Zhang, Jianmin Liu, Baohuan Su, Xuemin Liu, Guoli Qi and Yajun Ge, "Analysis of flow characteristics and flow measurement accuracy of elbow with different diameters", Earth and Environmental Science, 2018 ,113.

[10] M. Magnini A., Ullmann, N. Brauner and J.R.Thome,"Numerical study of water displacement from the elbow of an inclined oil pipeline", Journal of Petroleum Science and Engineering, 2018,166, 1000.

[11] Shi, J., Gourma, M., and Yeung, H., "CFD simulation of horizontal oil-water flow with matched density and medium viscosity ratio in different flow regimes". Journal of Petroleum Science and Engineering, 2017, 151, 373,.

[12] Issakhov, A., Bulgakov, R., and Zhandaulet, Y., "Numerical simulation of the dynamics of particle motion with different sizes. Engineering Applications of Computational Fluid Mechanics, 2018, 13,1.